

Chapter 5

Phase Behaviour of SDS-PTHC-Water System: An Unusual Phase Sequence from Hexagonal to Lamellar

5.1 Introduction

In previous chapters we have shown the influence of organic salts on the phase behaviour of cationic surfactants. In such systems, very rich phase diagrams consisting of many liquid crystalline phases have been observed. The appearance of mesh phases is a common feature in these systems. These systems are found to resemble in many ways the mixtures of two oppositely charged surfactants. In contrast, only a few systematic studies have been reported on the effects of organic salts on anionic surfactants, which suggest that these systems behave very similar to the cationic surfactant-organic salt systems in the low water content regime [1, 2, 3].

This chapter deals with the influence of the organic salt *p*-toluidine hydrochloride (PTHC) on the phase behaviour of the anionic surfactant sodium dodecylsulfate (SDS). Earlier studies on this system are described in section 5.2, which suggest that the addition of salt results in an increase in the length of the SDS cylindrical micelles at low surfactant concentrations. A short description of chemicals and experimental techniques has been given in section 5.3. The experimental results are described in section 5.4. Two important features, namely, the existence of a novel sponge phase and an unusual phase sequence from hexagonal to lamellar, have been observed. The ternary phase diagram is found to be asymmetric about the equimolar compositions of the two species. In section 5.5, plausible explanations of the appearance of different phases and the phase sequences

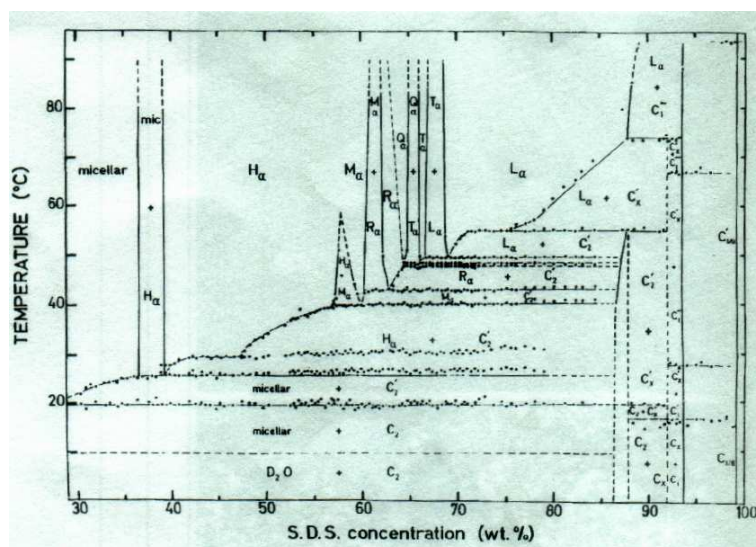


Figure 5.1: Phase diagram of SDS-water system. H_α , M_α , R_α , Q_α , T_α , L_α and C are the 2-D hexagonal, 2-D monoclinic, rhombohedral, cubic, tetragonal, lamellar and crystalline phases respectively [4].

are discussed. Finally, section 5.6 contains the conclusions that can be drawn from these studies.

5.2 Earlier Studies

The phase diagram of concentrated aqueous solutions of SDS has been determined in detail by Kekicheff et. al (Fig. 5.1) [4]. At very low concentration it shows an isotropic phase of cylindrical micelles, and a two dimensional (2-D) hexagonal phase is observed over a wide range of intermediate surfactant concentrations. Before forming the lamellar phase at very high concentrations it shows a number of intermediate phases over narrow ranges of surfactant concentrations. This is an excellent example of a surfactant-water system, where intermediate phases are seen as morphological intermediaries between the 2-D hexagonal and 1-D lamellar phases.

Aqueous mixtures of oppositely charged surfactants exhibit very interesting properties due to the strong electrostatic interactions between their head groups. At very low concentrations, the length of rod-like SDS micelles has been seen to grow upon the addition of the cationic surfactant dodecyltrimethylammonium bromide (DTAB). These rod-like micelles are found to transform into vesicle over a narrow composition range [5]. The phase behaviour at much higher concentrations is dominated by different liquid crystalline phases [6]. The effect of octyltrimethylammonium

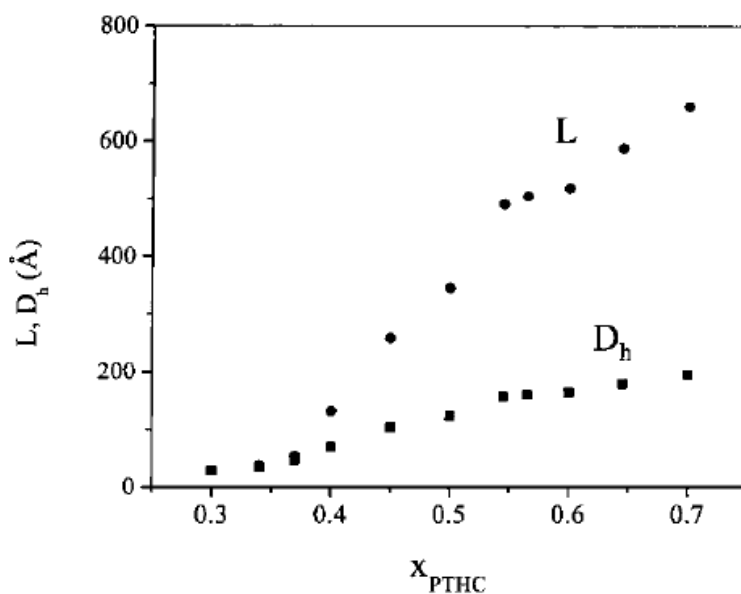


Figure 5.2: Average length of SDS rodlike micelles (L) and the average equivalent sphere hydrodynamic diameter as a function of the molar ratio of PTHC [1].

bromide (OTAB) on SDS system has also been reported in [7].

Instead of a cationic surfactant, Hassan and co-workers have used some organic cationic counterions to tune the microstructure of the SDS cylindrical micelles [1, 2]. They found the growth of SDS micelles as a function of added *p*-toluidine hydrochloride (PTHC) in the very dilute regime (< 5 wt%) (Fig. 5.2). NMR studies have revealed that the counterions are adsorbed at the micelle-water interface with its aromatic ring intercalated in the hydrophobic interior of the micelles. It reduces the effective charge density at the micellar surface and hence, there is a shift of the microstructure to those with lower mean curvature. Changing the position of the methyl substitute in the benzene ring of the aromatic salt to ortho and meta positions, the growth of the micelle is found to be different. Dynamic light scattering (DLS) studies have shown that PTHC and *m*-toluidine hydrochloride (MTHC) induce much longer micelles than aniline hydrochloride (AHC) and *o*-toluidine hydrochloride (OTHC) at similar salt concentrations [3].

5.3 Experimental

Sodium dodecylsulfate (SDS) (99% purity) and *p*-toluidine hydrochloride (PTHC) (98% purity) were purchased from Aldrich and were used without further purification. The chemical structures

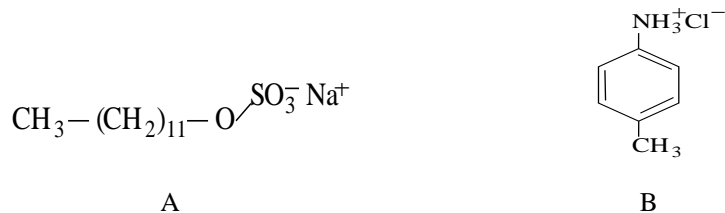


Figure 5.3: Chemical structure of (A) sodium dodecyl sulfate and (B) *p*-toluidine hydrochloride.

of the molecules are shown in figure 5.3. Samples were prepared in the same way as described in the previous chapters.

Different phases were identified using polarizing optical microscopy (POM) and X-ray diffraction as described in previous chapters.

5.4 Results

The phase behaviour of mixtures of SDS and PTHC was studied at different values of the molar ratio ($\alpha = \frac{[PTHC]}{[SDS]}$) of the two components. For each α the total concentration of the non-aqueous components ($\phi_s = \frac{(SDS+PTHC)}{(SDS+PTHC+water)} \times 100\%$) was varied from 10% to 80%. The microscopy texture of each sample was monitored from 30 to 80 °C. The structure of the phases was confirmed using diffraction studies. To construct the three component phase diagram around 100 samples were studied.

5.4.1 Phase behaviour at $\alpha < 1$

The phase behaviour of the SDS-water system in the presence of small amounts of added PTHC salt is found not to be different from that of the pure system. For $\alpha < 0.15$, at low ϕ_s (< 30) there exists an isotropic phase which shows birefringence under shear. At higher ϕ_s the diffraction patterns show three peaks with the corresponding spacings in the ratio $1:\frac{1}{\sqrt{3}}:\frac{1}{2}$ confirming the 2-D hexagonal structure, as in the system without salt.

For $\alpha = 0.25$, at low surfactant concentration ($\phi_s \leq 30$) an isotropic phase is found which does not show flow birefringence (Fig. 5.4). On increasing ϕ_s a nematic phase appears which shows the typical thread-like texture under the microscope. The texture contains large pseudo-isotropic patches where the nematic director aligns perpendicular to the substrate (Fig. 5.5). This phase

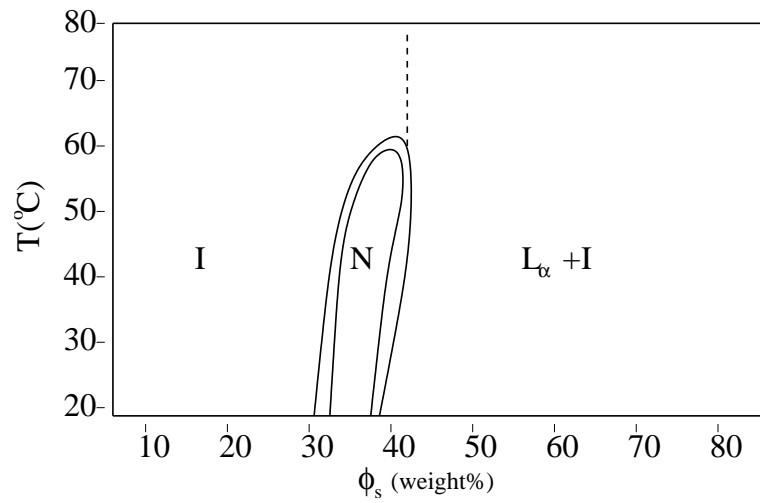


Figure 5.4: Phase diagram of SDS-PTHC-water system at $\alpha = 0.25$. I , N and L_α denote the isotropic, nematic and lamellar phases, respectively. The dashed line refers to the phase boundary which is not determined precisely.



Figure 5.5: Texture of the nematic phase under crossed polarizer at $\alpha = 0.25$, $\phi_s = 40$ and $T = 45^\circ\text{C}$. Dark patches correspond to regions where the optic axis of the medium is aligned normal to the substrate.

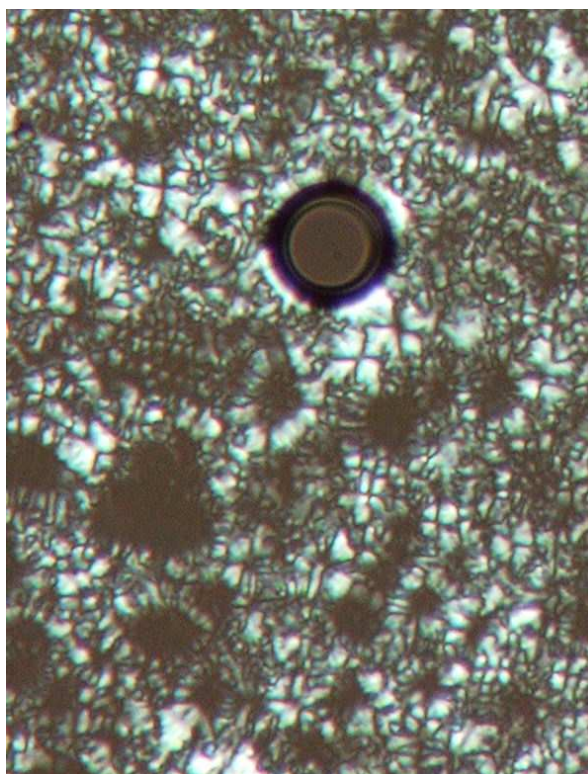


Figure 5.6: Texture of the lamellar phase under crossed polarizers in SDS-PTHC-water system.

goes to an isotropic phase on increasing the temperature through a two phases region. On further increasing of ϕ_s , a complex is formed which precipitates out leaving an isotropic solution. The complex shows the oily streak texture which is the characteristic texture of a lamellar phase (Fig. 5.6). The coexistence of the lamellar and isotropic phases is found over a wide range of surfactant concentrations. The lamellar phase first transforms into a nematic and then to an isotropic phase on heating at $\phi_s = 40$ (Fig. 5.7). The diffraction pattern of the nematic phase shows a diffuse peak, whereas that of the lamellar phase shows sharp peaks with the corresponding spacings in the ratio $1:\frac{1}{2}:\frac{1}{3}$ (Table 5.1).

At $\alpha = 0.5$, for low ϕ_s an isotropic phase is found. The nematic phase is not observed at this salt concentration. The uniform isotropic phase transforms to a isotropic-lamellar coexistence region (Fig. 5.8) at higher ϕ_s . At $\alpha = 0.75$, this coexistence region is found for all values of ϕ_s .

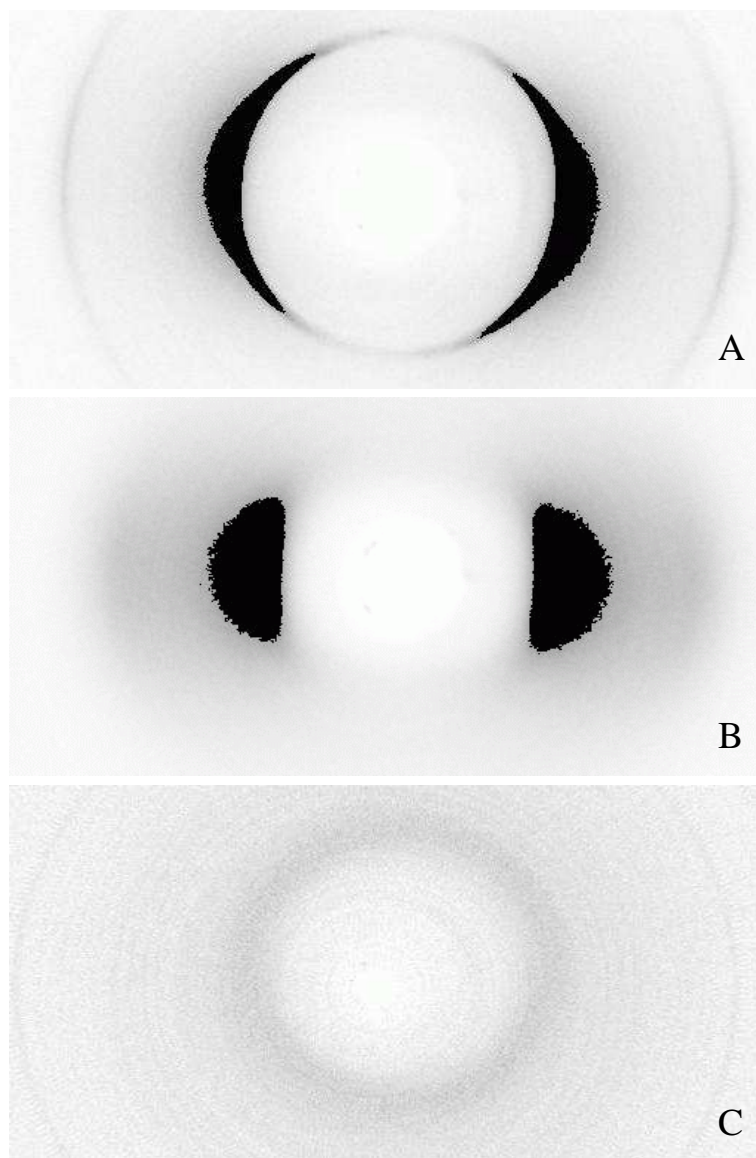


Figure 5.7: X-ray diffraction patterns of (A) lamellar (L_α), (B) nematic (N) and (C) isotropic (I) phases in SDS-PTHC-water system at $\alpha = 0.25$ and $\phi_s = 40$. The phases have been observed on heating at 23, 45 and 60 °C respectively.

Table 5.1: The d-spacings and polarizing optical microscopy textures of the different mesophases in SDS-PTHC-water system at $\alpha = 0.25$ and $T = 30$ °C.

ϕ_s	d_1 (nm)	d_2 (nm)	d_3 (nm)	POM	phase
30	very diffuse	-	-	isotropic	I
35	4.9	-	-	nematic texture	N
40	4.58	-	-	nematic texture	N
45	3.78	1.9	1.29	oily streak texture	$I + L_\alpha$
50	3.7	1.86	-	oily streak texture	$I + L_\alpha$
60	3.53	1.78	1.20	oily streak texture	$I + L_\alpha$
70	3.4	-	-	oily streak texture	$I + L_\alpha$

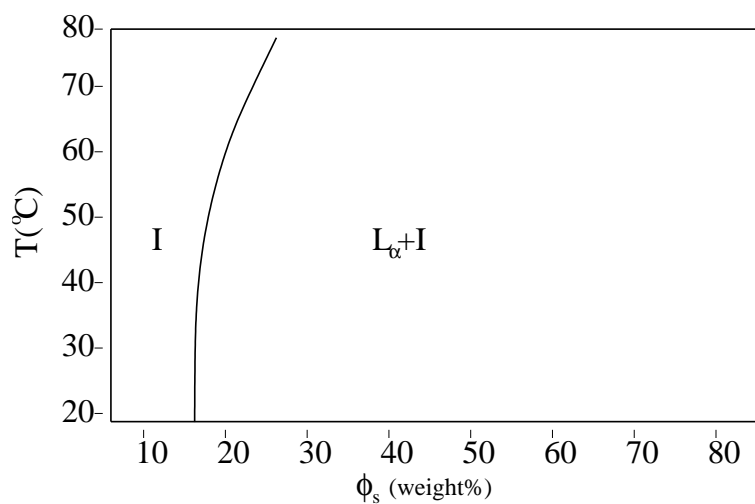


Figure 5.8: Phase diagram of the SDS-PTHC-water system at $\alpha = 0.5$.

Table 5.2: Variation of the lamellar periodicity (d) with ϕ_s in the SDS-PTHC-water system at $\alpha = 1$ and $T = 30^\circ\text{C}$.

ϕ_s	$d(\text{nm})$	$phase$
30	5.38	L_α
40	4.30	L_α
50	4.06	L_α
60	4.06	L_α
70	3.84	L_α

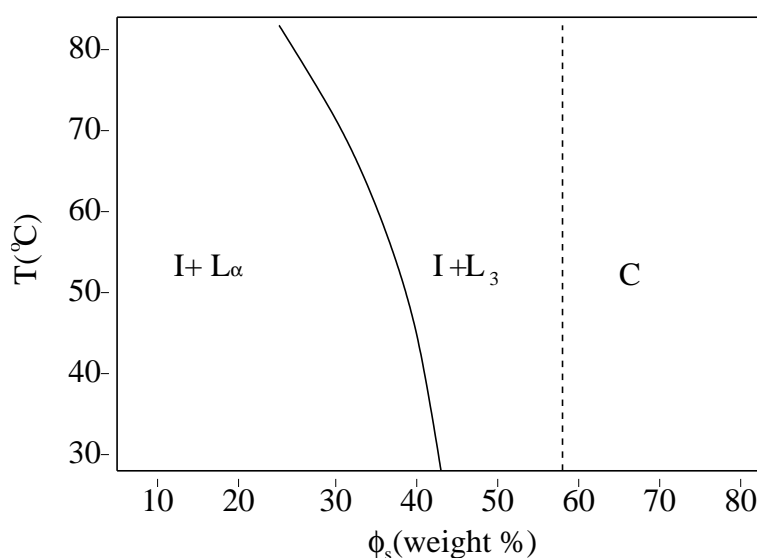


Figure 5.9: Phase diagram of SDS-PTHC-water system at $\alpha = 1.25$. I , L_α , L_3 and C denote the isotropic, lamellar, sponge and crystalline phases respectively.

5.4.2 Phase behaviour at $\alpha \approx 1$

Near equimolar ratio of the two components, a complex is always found to form over the whole surfactant concentrations, which precipitates out of the solution leaving an isotropic phase at the top. This complex shows the typical oily streak texture of the lamellar phase. In this system, the lamellar spacings are found to be low (Table 5.2 & 5.3) which indicates that the bilayers do not swell much. It is to be noted that there is no diffuse peak found in the direction normal to the lamellar periodicity (Fig. 5.7A).

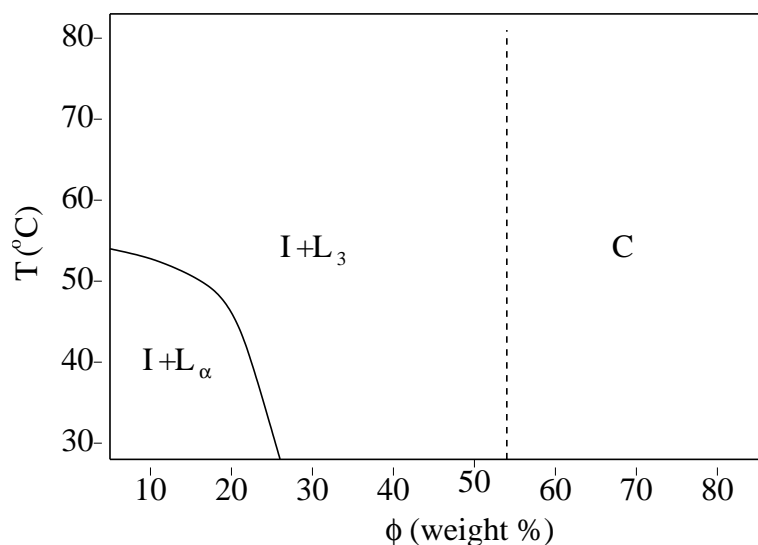


Figure 5.10: Phase diagram of SDS-PTHC-water system at $\alpha = 1.5$.

5.4.3 Phase behaviour at $\alpha > 1$

At low ϕ_s , a precipitate is found which coexists with an isotropic phase. The precipitate is found to show typical lamellar texture under polarizing microscope. On addition of more surfactants, the sample is found to show the coexistence of two isotropic phases (Fig. 5.9 & 5.10).

The two isotropic phases are found to phase separate with a very clear meniscus at low ϕ_s whereas at higher values the meniscus is not sharp (Fig. 5.11). Under polarizing microscope, the appearance of the second isotropic phase (L_3) from L_α was clearly observed with increasing temperature. The X-ray diffraction studies show a very sharp peak from the L_α phase, whereas in the L_3 phase it becomes very diffuse (Fig. 5.12). The interbilayer separation in the lamellar phase and the average separation in the L_3 phase are found to be similar. At higher ϕ_s , PTHC is found to crystallize out from the sample.

With increasing salt concentration, the L_α phase is found over a narrower range of surfactant concentration and temperature. At much higher α values, this phase disappears, and the coexistence of L_3 and I phases is found over a wide range of surfactant concentration (Fig. 5.13). Further, the phase boundary between the L_3 and C phases is found to shift to lower values of ϕ_s .

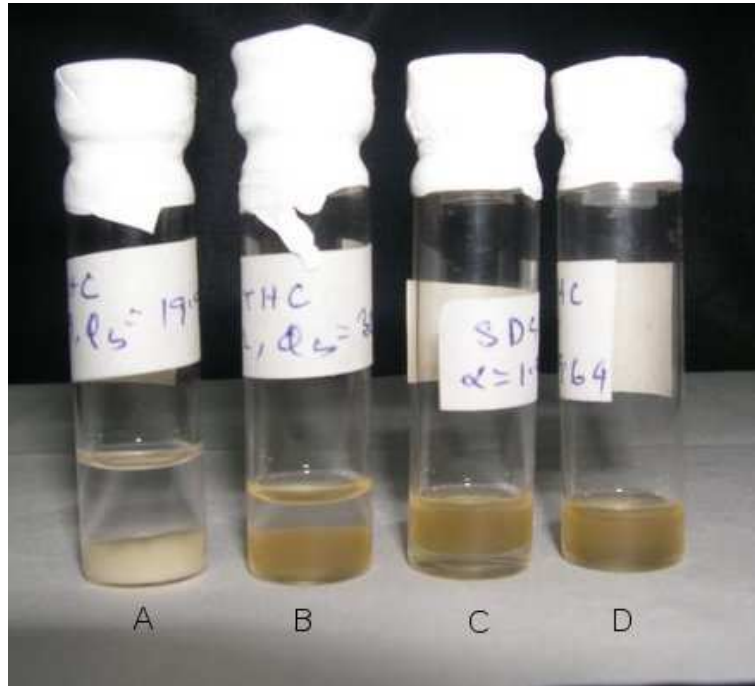


Figure 5.11: The different phases in SDS-PTHC-water system at $\alpha = 1.5$ and $T = 30^\circ\text{C}$; (A) whitish precipitate of L_α phase at the bottom along with an isotropic phase (I) floating at the top at $\phi_s = 20$, (B) isotropic-isotropic coexistence at $\phi_s = 30$, where L_3 is at the bottom and I at the top, (C) L_3 floats on the top of I at $\phi_s = 40$, (D) no sharp meniscus between L_3 and I at $\phi_s = 50$.

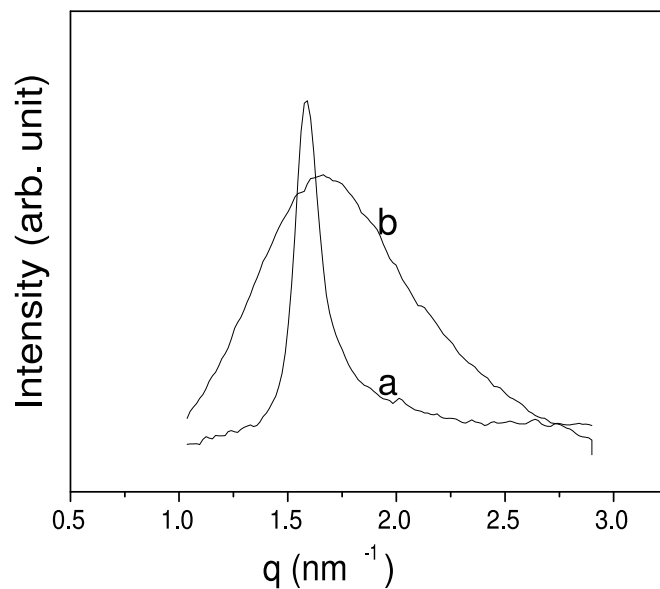


Figure 5.12: X-ray diffraction patterns of SDS-PTHC-water system at $\alpha = 1.25$ and $\phi_s = 30$ (a) and $\phi_s = 50$ (b) corresponding to L_α and L_3 phases respectively.

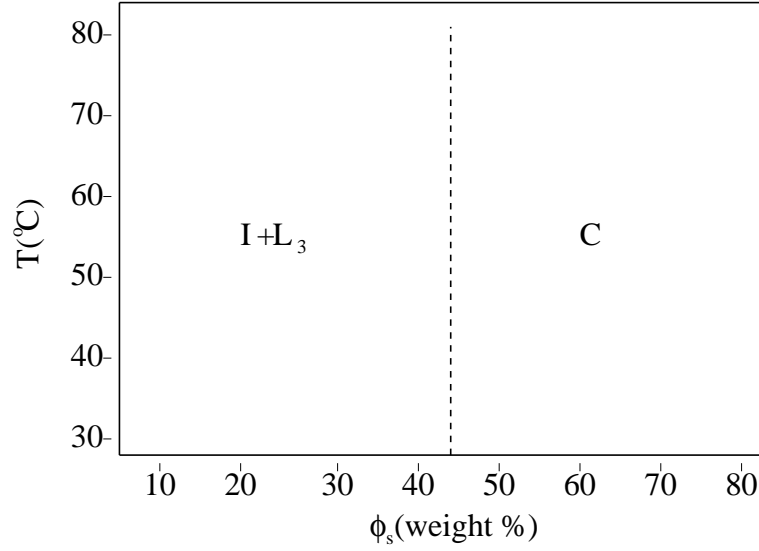


Figure 5.13: Phase diagram of SDS-PTHC-water system at $\alpha = 2.5$. At this high amount of added salt the L_3 phase is stabilized over the L_α phase.

Table 5.3: The lamellar periodicity (d) and the average spacings (D) for L_α and L_3 phases respectively in SDS-PTHC-water system at $T = 30^\circ\text{C}$.

α	ϕ_s	phase	$d/D(\text{nm})$
1.25	30	L_α	3.95
1.25	40	L_α	3.95
1.25	50	L_3	3.78
1.5	20	L_α	4.35
1.5	40	L_3	3.89

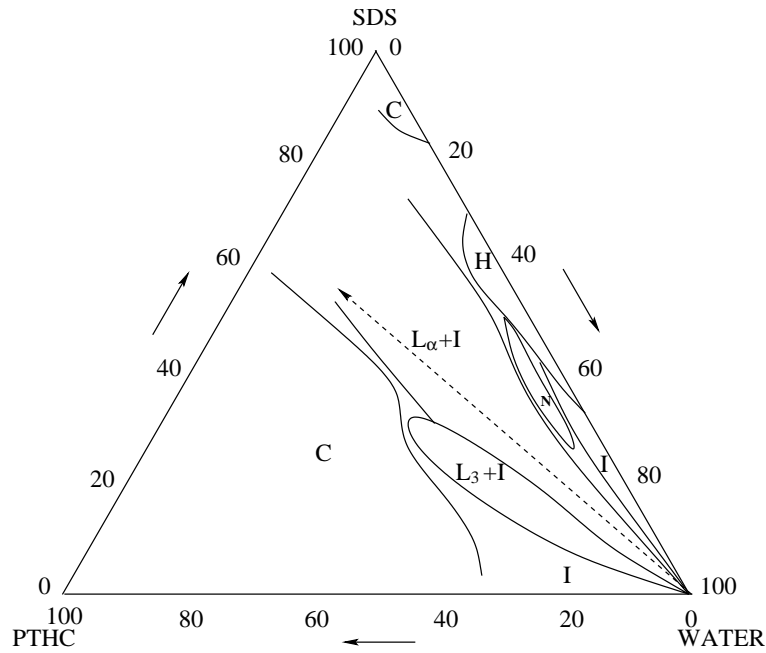


Figure 5.14: Partial ternary phase diagram of SDS-PTHC-water system at 30 °C. The concentrations are in wt%. *I*, *N*, L_α , *H*, L_3 and *C* denote the isotropic, nematic, lamellar, hexagonal, sponge and crystalline phases respectively. The dashed arrow indicates the equimolar compositions of SDS and PTHC.

5.4.4 Ternary phase diagram

The three component phase diagram at 30 °C is shown in figure 5.14. It is dominated by a lamellar-isotropic coexistence region. Interestingly, the phase diagram is not symmetric about the line of equimolar composition of SDS and PTHC, unlike that of the CTAB-SHN-water system discussed in chapter 2. At $\alpha < 1$, there are a number of mesophases present. On the other hand, for $\alpha > 1$, only the lamellar-isotropic and L_3 -isotropic regions are seen; the nematic and hexagonal phases are absent in this part of the phase diagram.

5.5 Discussion

5.5.1 Nematic and lamellar phases

An isotropic phase made up of long rod-like micelles shows flow birefringence because of the flow induced orientational ordering. At very low surfactant and salt concentrations, the isotropic phase found in the present system shows such flow birefringence, indicating the presence of long cylindrical micelles. But for $\alpha > 0.2$, the isotropic phase does not show such a behaviour for $\phi_s \leq 30$.

Further the nematic phase formed at higher values of ϕ_s shows some pseudo-isotropic patches under cross polarizers, where the optic axis is normal to the glass plates. These observations suggest that the isotropic and the nematic phases at these compositions are made up of disc-like aggregates. It is very natural for disc-like micelles to align parallel to the substrates, so that the optic axis of the nematic medium is normal to the boundaries. On the other hand, it would require rod-like micelles to align with their long axes normal to the substrates, which is extremely unlikely. The transition from lamellar to nematic, and then to isotropic on heating further supports the possible presence of disc-like aggregates. This kind of phase transition on heating has been observed in caesium pentadecafluoro-octanoate (CsPFO) - water system where the nematic phase is well established to be made up of disc-like micelles [8, 9, 10].

The lamellar phase found at all the compositions in this system coexists with an isotropic phase. The bilayer does not swell much on dilution (Table 5.3), which can be understood in terms of the screening of the electrostatic interaction between the bilayers. At any value of α , increasing ϕ_s increases the concentration of dissociated Na^+ and Cl^- ions in the solution. The electrostatic potential of the bilayer is given by [11],

$$\psi_x = \psi_0 e^{-kx} \quad (5.1)$$

where ψ_0 is the potential at the bilayer surface and $\frac{1}{k}$ is the Debye length. This is the characteristic decay length of the potential. At 25 °C the Debye length of aqueous solutions can be written as,

$$\frac{1}{k} = \frac{0.304}{\sqrt{C}} \quad (5.2)$$

for 1:1 electrolytes. C is the molar concentration of salt.

The presence of large amounts of dissociated salt in the present system makes the Debye length extremely short (Table 5.4). This can qualitatively explain the low values of the lamellar spacing observed in this system.

Table 5.4: Variation of Debye length ($\frac{1}{k}$) in the presence of the dissociated NaCl salt in the SDS-PTHC-water system at $\alpha = 1$ and $T = 25$ °C. $C[M]$ is the molar concentration of the salt.

ϕ_s	$C[M]$	$\frac{1}{k}(nm)$
30	0.99	0.3
40	1.54	0.245
50	2.315	0.199
60	3.47	0.163
70	5.4	0.131

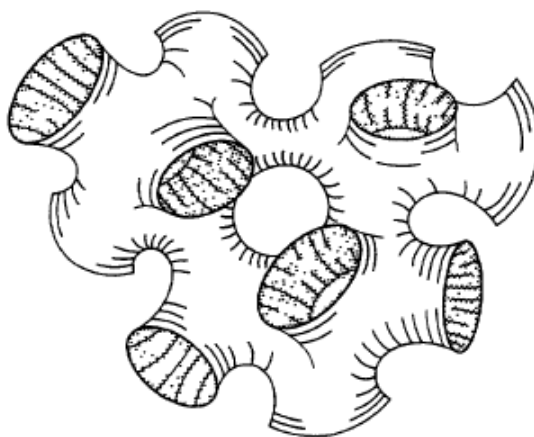


Figure 5.15: Schematic picture of the classical sponge phase (L_3) [18].

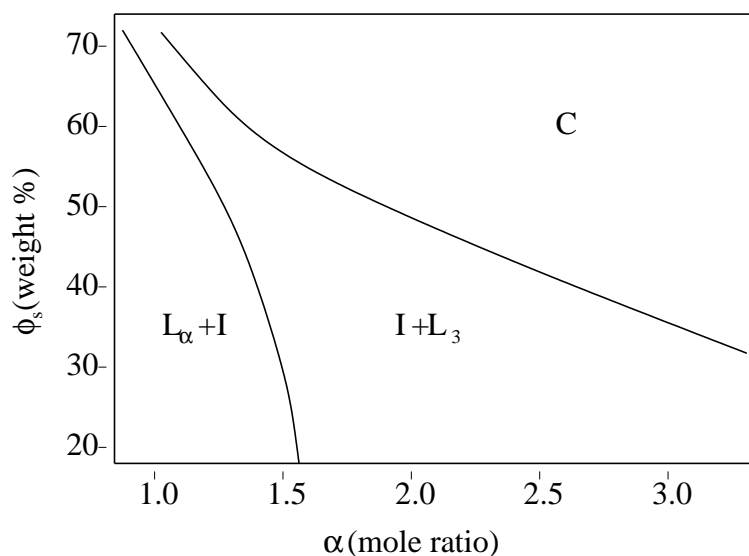


Figure 5.16: Phase diagram of SDS-PTHC-water system at 30° C. There is no two-phase region at the L_α to L_3 phase transition.

5.5.2 The L_3 phase

The classical sponge phase (L_3) was first discovered by Lang and Morgan in the $C_{10}E_4$ -water system in 1980 [12]. Since then it has been observed in many nonionic, ionic and block copolymer systems [13, 14]. This phase can be considered as a molten lamellar (L_α) phase existing at high dilution. It is a bicontinuous phase where the network of bilayers separate the aqueous region into two disconnected parts (Fig. 5.15) [15]. The structure of this phase has been deduced by different experimental techniques, such as, small angle x-ray and neutron scattering [16, 17], light scattering [18], and ionic conductivity measurements [19]. Freeze-fracture transmission electron microscopy (FF-TEM) studies have given direct visual evidence of its multiply connected bilayer structure [20, 21].

Figure 5.16 shows the phase behaviour of the system at 30° C in the $\alpha - \phi_s$ plane. Generally the classical L_3 phase appears from the L_α phase via a narrow two phase region (Fig. 5.17). In the present system an $L_\alpha - L_3$ two-phase region is not found either on changing ϕ_s or temperature. Normally the x-ray diffraction pattern of the L_3 phase shows a broad peak at around $q_0/3$, where q_0 is the position of the sharp peak from the neighbouring L_α phase [22, 23]. However, in the present system the positions of the two peaks are almost identical (Fig. 5.12). Similar behaviour has been

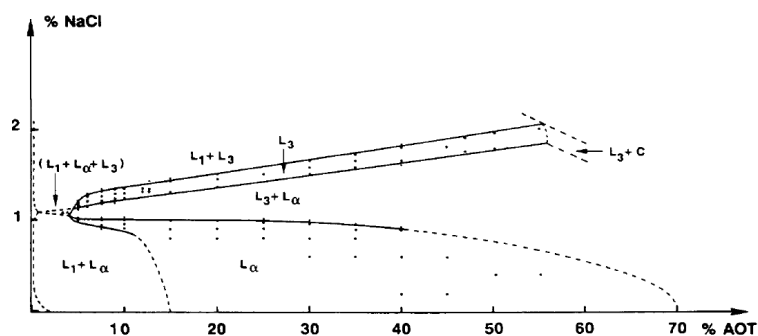


Figure 5.17: Phase diagram of $AOT - NaCl - D_2O$ system. There is a two phase region between the L_α and L_3 phases [18].

recently reported for the L_3 phase in the calcium tetradecylmethylester- α -sulfonate ($Ca(C_{14} - \alpha MES)_2$) - water and the 2-ethylhexyl-monoglycerinether (EHG) - water systems [23, 24]. Ionic conductivity measurements and FF-TEM micrographs showed typical features of the L_3 phase in these systems but with two important differences from classical L_3 phases, namely, a continuous $L_\alpha \rightarrow L_3$ transition and similar q-values of the diffraction peaks from these two phases (Fig. 5.18). Due to these differences, in references [23, 24] this phase has been referred to as a “novel L_3 ” phase. A similar phase behaviour has been reported by the same group in calcium dodecylsulfate in the presence of the cosurfactant 1-phenylpropyl-amine [23]. Since the sponge phase in the present system also exhibits the above mentioned two differences from classical sponge phases, it might be another example of the “novel L_3 ” phase. Further experiments are necessary to figure out how the microstructure of this phase is different from that of the classical sponge phase.

5.5.3 Phase transition from hexagonal to lamellar

The phase transition from 2-D hexagonal to 1-D lamellar is accompanied by changes in the aggregate morphology from cylindrical micelles with uniform positive interfacial mean curvature to bilayers with zero curvature. In some systems intermediate phases or bicontinuous cubic phases are found between these two phases as discussed in the previous chapters.

Present investigations have revealed an unusual transition route from hexagonal to lamellar in the SDS-PTHC-water system:

2-D hexagonal \rightarrow *Nematic* \rightarrow *Isotropic* \rightarrow *Nematic* \rightarrow *1-D Lamellar*.

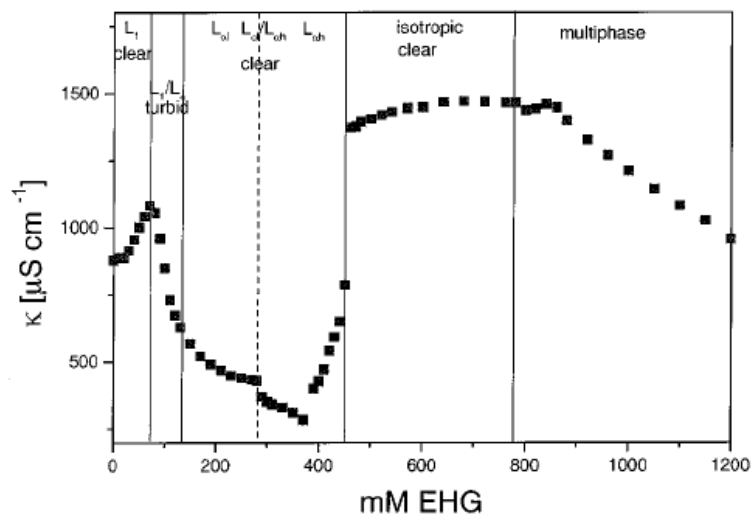


Figure 5.18: Variation of the ionic conductivity of a 50mM aqueous solution of $Ca(C_{14} - \alpha MES)_2$ with the addition of the cosurfactant EHG at 25°C. Note the absence of a two phase region between the L_α and L_3 phases [21].

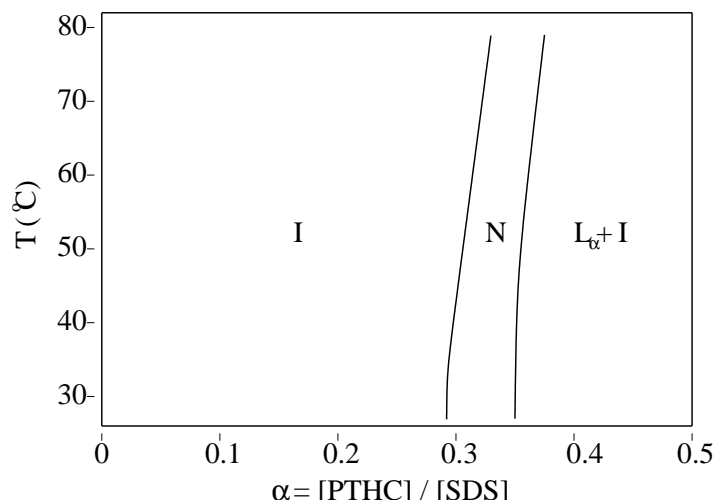


Figure 5.19: The T - α phase diagram of SDS-PTHC-water system at $\phi_s = 30$.

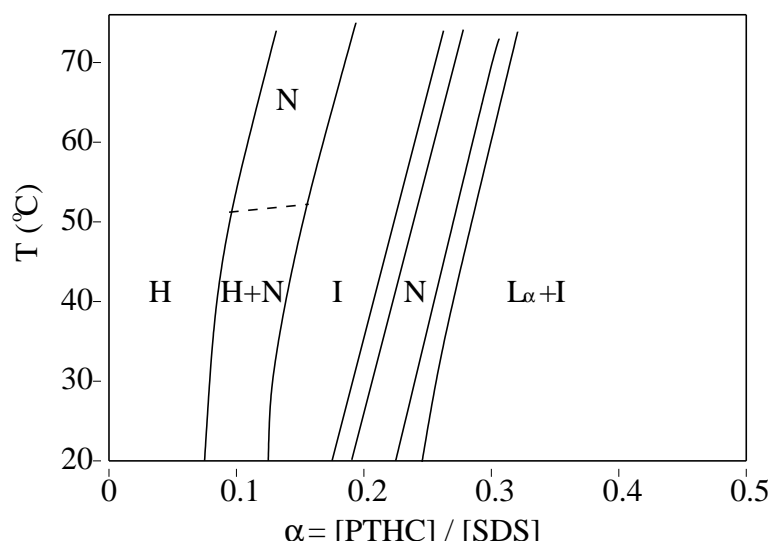


Figure 5.20: The T - α phase diagram of SDS-PTHC-water system at $\phi_s = 40$.

The two nematic phases are made up of rod-like and disc-like aggregates, respectively. Figures 5.19 and 5.20 show the phase behaviour at fixed ϕ_s as a function of temperature and PTHC concentration. At lower ϕ_s where the system is initially in an isotropic phase of cylindrical micelles, the isotropic phase goes to a nematic and then to a lamellar phase on increasing PTHC concentration. It is seen that the scattering intensity profile of the isotropic phase near the nematic and far away from it are different (Fig. 5.21), which suggests that the microstructures of the aggregates at these two compositions might be very different. At higher ϕ_s , where the system is initially in the 2-D hexagonal phase made up of cylindrical micelles, an isotropic phase is induced between two nematic phases on the addition of salt. The nematic near the hexagonal phase is most probably made up of rod-like aggregates, whereas the one near the lamellar phase is likely to consist of disc-like micelles. The observed phase sequence suggests that the isotropic phase is made up of almost spherical aggregates. The phase sequence is consistent with a gradual transformation of the aggregate shape from cylindrical to disc-like with increasing PTHC concentration (Fig. 5.22). The apparent viscosity of the samples shows a monotonic decrease within the hexagonal phase with increasing PTHC concentration, again indicating a gradual decrease in the length of the cylindrical micelles making up this phase.

Usually the addition of organic salts to a dispersion of rod-like aggregates is found to increase the length of the rods significantly, resulting in long worm-like micelles. But in the present system

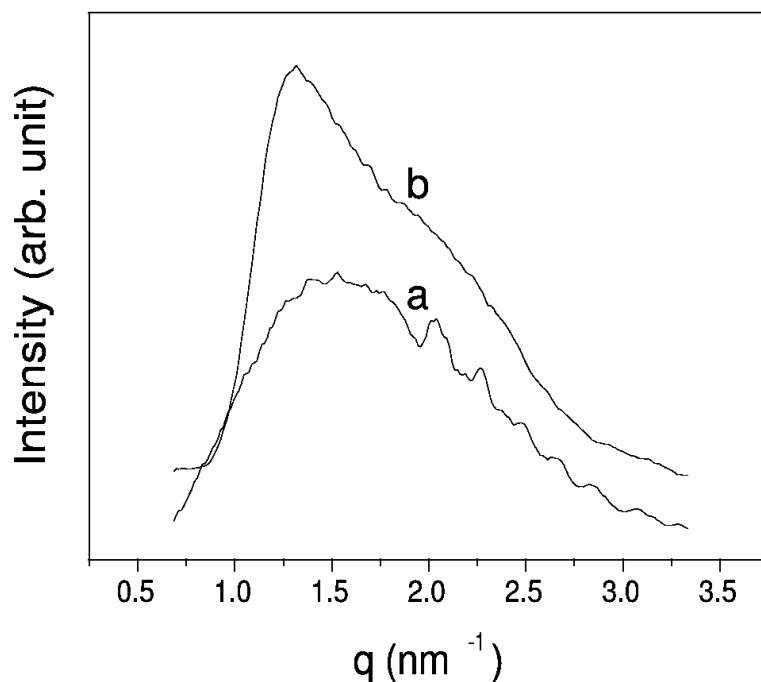


Figure 5.21: The intensity profile from the isotropic phase at $\phi_s = 30$ and (a) $\alpha = 0.126$ and (b) $\alpha = 0.254$ at 30°C .

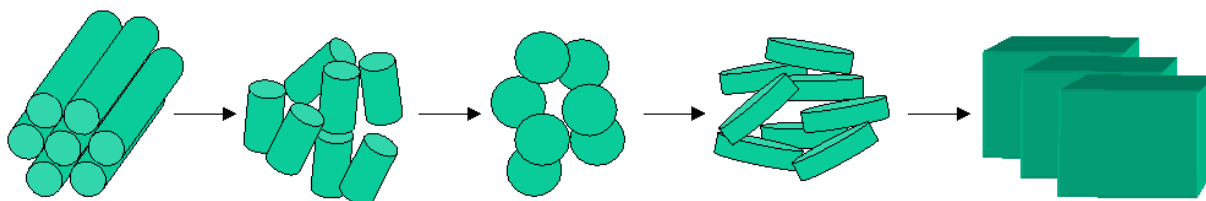


Figure 5.22: Schematic drawing of the proposed changes in the SDS aggregate morphology with increasing PTHC concentration.

it seems that the addition of salt decreases the length of the rod like aggregate. It is presently not clear if this behaviour is specific to PTHC or if it is more general. Further experiments are needed to clarify the situation.

5.5.4 Asymmetric ternary phase diagram

In mixtures of oppositely charged surfactants, it is very common to get a ternary phase diagram, which is symmetric about the line of the equimolar composition of the charged species (Fig. 5.23) [5, 25]. On each side of the equimolar line, the aggregates are either charged positively or negatively. The morphology of the aggregates usually depends only on the charge density but not on the type of the charge; with bilayers preferred close to the equimolar composition and cylindrical

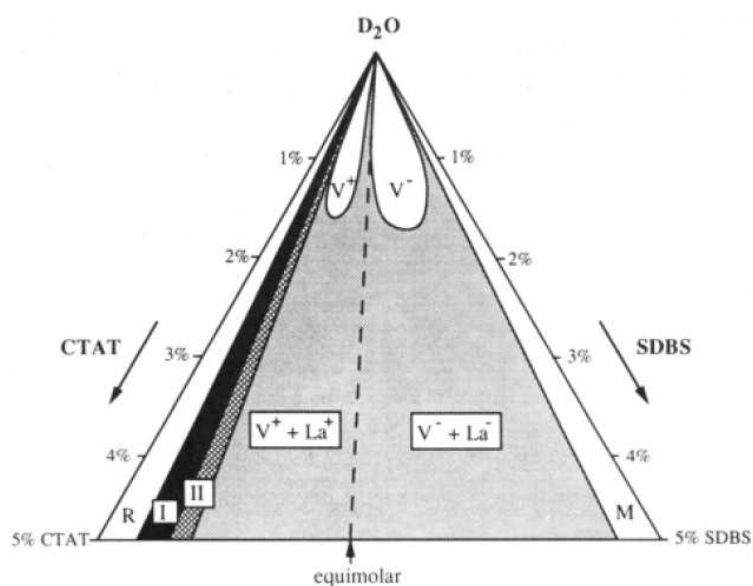


Figure 5.23: Ternary phase diagram of $CTAT-SDBS-D_2O$ system at $28^\circ C$ [25]. M and R are the SDBS and CTAT rich micelles whereas V and L_α are the vesicle and lamellar phase, respectively. The CTAT and SDBS rich phases are indicated '+' and '-'.

micelles away from it. Hence, the phase behaviour is usually symmetric about the equimolar axis. Strongly bound counterions, which are very weakly soluble in water, seem to behave similar to ionic surfactants. In chapters 2 and 4, it has been reported that the addition of strongly bound anionic counterions to some cationic surfactants shows similar behaviour [26]. However, this is not the case in the present system. A possible reason might be that PTHC is reasonably soluble in water, unlike SHN which was added to the cationic system. This can destroy the symmetry of the aggregate charge density about the equimolar composition, thus giving rise to an asymmetric ternary phase diagram. Further experiments are needed to confirm this conjecture.

5.6 Conclusion

The influence of the strongly bound cationic counterion PTH^+ on the phase behaviour of concentrated aqueous solutions of the anionic surfactant SDS was studied using x-ray diffraction and polarizing optical microscopy. On increasing the concentration of the counterion the hexagonal phase of SDS is found to show the following sequence of transformations: hexagonal \rightarrow nematic \rightarrow isotropic \rightarrow nematic \rightarrow lamellar. This sequence of phases suggests a gradual prolate to oblate

change in the aggregate morphology with increasing counterion concentration. Such a morphological change seems to prevent the formation of other intermediate phases usually seen between the hexagonal and lamellar. At much high amount of PTHC, an isotropic-isotropic coexistence is observed. One of these is tentatively identified as a sponge phase, which seems to be different from the classical sponge phase in some respects. Further, the ternary phase diagram is asymmetric about the equimolar line of the charged components, unlike those of the systems described in chapters 2 and 4 and in the case of mixtures of anionic and cationic surfactants.

Bibliography

- [1] P. A. Hassan, S. R. Raghavan and W. Kaler *Langmuir*, **18**, 2543 (2002).
- [2] P. A. Hassan, G. Fritz and E. W. Kaler *J. Colloid Int. Sci*, **257**, 154 (2003).
- [3] G. Garg, P. A. Hassan, V. K. Aswal and S. K. Kulshrestha *J. Phys. Chem*, **109**, 1340 (2005).
- [4] P. Kekicheff and B. Cabane *Acta Cryst*, **44**, 395 (1988).
- [5] K. L. Herrington, E. W. Kaler, D. D. Miller, J. A. Zasadzinski and S. Chiruvolu *J. Phys. Chem*, **97**, 13792 (1993).
- [6] D. H. Chen and D. G. Hall *Kolloid-Z. Z. Polym*, **262**, 41 (1973).
- [7] C. A. Barker, D. Saul, G. J. T. Tiddy, B. A. Wheeler and E. Willis *J. Chem. Soc., Faraday Trans. I*, **70**, 154 (1974).
- [8] M. S. Leaver and M. C. Holmes *J. Phys. II France*, **3**, 105 (1993).
- [9] M. C. Holmes, A. M. Smith and M. S. Leaver *J. Phys. II France*, **3**, 1357 (1993).
- [10] M. C. Holmes, P. Sotta, Y. Hendrix and B. Deloche *J. Phys. II France*, **3**, 1735 (1993).
- [11] J. Israelachvili *Intermolecular and Surfaces Forces*, 2nd edition, Academic Press, London (1991).
- [12] J. Lang and R. D. Morgan *J. Chem. Phys.*, **73**, 5849 (1993).
- [13] M. Jonstromer and R. Strey *J. Phys. Chem*, **96**, 5993 (1992).
- [14] E. Hecht, K. Mortensen and H. Hoffmann *Macromolecules*, **28**, 5465 (1995).

- [15] M. Cates, D. Roux, D. Andelman, S. C. Milne and S. Safran *Europhys Lett*, **5**, 733 (1988).
- [16] D. Gazeau, A. M. Bellocq, D. Roux and T. Zemb *Europhys Lett*, **9**, 447 (1989).
- [17] R. Strey, R. Schomacker, D. Roux, F. Nallet and U. Olsson *J. Chem Soc Faraday Trans*, **86**, 2253 (1990).
- [18] M. Skouri, J. Marignan, J. Appel and G. Porte *J. Phys II*, **1**, 1121 (1991).
- [19] K. Fukuda, U. Olsson and U. Wurz *Langmuir*, **10**, 3222 (1994).
- [20] H. Hoffmann, C. Thuning, U. Munkert, H. W. Meyer and W. Richter *Langmuir*, **8**, 2629 (1992).
- [21] R. Beck and H. Hoffmann *Phys. Chem. Chem. Phys*, **3**, 5438 (2001).
- [22] G. Porte, J. Appell, P. Bassereau and J. Marignan *J. Phys. France*, **50**, 1335 (1989).
- [23] R. Beck and H. Hoffmann in *Bicontinuous Liquid Crystals*, Edited by M. L. Lynch and P. T. Spicer, Taylor and Francis, USA (2005).
- [24] R. Beck and H. Hoffmann *J. Phys. Chem. B*, Vol **106**, No. 13, 3337 (2002).
- [25] E.W. Kaler, K. L. Herrington, A. K. Murthy and J. A. N. Zasadzinski *J. Phys. Chem*, **96**, 6698 (1992).
- [26] R. Krishnaswamy, S. K. Ghosh, S. Laksmanan, V. A. Raghunathan and A. K. Sood *Langmuir*, **21**, 10439 (2005).